⌘ *Author's Choice*

G Protein-coupled Receptor Kinases Phosphorylate LRP6 in the Wnt Pathway*[S]

Minyong Chen[‡1], **Melanie Philipp**[§1,2], **Jiangbo Wang**[‡], **Richard T. Premont**[‡], **Tiffany R. Garrison**[‡], **Marc G. Caron**[‡§], **Robert J. Lefkowitz**[‡¶‖3], **and Wei Chen**[‡4]

From the Departments of ‡Medicine, §Cell Biology, and ¶Biochemistry and the ‖Howard Hughes Medical Institute, Duke University Medical Center, Durham, North Carolina 27710

Wnt ligands conduct their functions in canonical Wnt signaling by binding to two receptors, the single transmembrane low density lipoprotein receptor-related proteins 5 and 6 (LRP5/6) and seven transmembrane (7TM) Frizzled receptors. Subsequently, phosphorylation of serine/threonine residues within five repeating signature PPPSP motifs on LRP6 is responsible for LRP6 activation. GSK3β, a cytosolic kinase for phosphorylation of a downstream effector β-catenin, was proposed to participate in such LRP6 phosphorylation. Here, we report a new class of membrane-associated kinases for LRP6 phosphorylation. We found that G protein-coupled receptor kinases 5 and 6 (GRK5/6), traditionally known to phosphorylate and desensitize 7TM G protein-coupled receptors, directly phosphorylate the PPPSP motifs on single transmembrane LRP6 and regulate Wnt/LRP6 signaling. GRK5/6-induced LRP6 activation is inhibited by the LRP6 antagonist Dickkopf. Depletion of GRK5 markedly reduces Wnt3A-stimulated LRP6 phosphorylation in cells. In zebrafish, functional knock-down of GRK5 results in reduced Wnt signaling, analogous to LRP6 knock-down, as assessed by decreased abundance of β-catenin and lowered expression of the Wnt target genes *cdx4*, *vent*, and *axin2*. Expression of GRK5 rescues the diminished β-catenin and *axin2* response caused by GRK5 depletion. Thus, our findings identify GRK5/6 as novel kinases for the single transmembrane receptor LRP6 during Wnt signaling.

Wnt molecules are secreted extracellular signaling ligands conserved from worms to humans, which regulate organogenesis and tissue regeneration. On the surface of target cells, Wnts directly bind to and activate two structurally unrelated co-receptors: the single transmembrane receptors low density lipoprotein receptor-related proteins 5 and 6 (LRP5 and LRP6)[5] and seven transmembrane (7TM) receptors of the Frizzled family (1–4). Both receptors act in concert to inhibit the kinase activity of cytosolic glycogen synthase kinase-3β (GSK3β), which leads to stabilization of β-catenin in the cytosol and enhances the nuclear activity of LEF/TCF transcription factors (5, 6). Abnormal Wnt/LRP5/6 signaling has been associated with many types of cancers and stem cell-related developmental diseases (7).

Upon Wnt3A stimulation, LRP6 is activated by phosphorylation at its C terminus. The phosphorylation sites include 1) threonine 1479 phosphorylated by the membrane-associated casein kinase 1γ (8), and 2) multiple serine/threonine residues within five repeating signature PPPSP motifs, which are typically monitored by phosphorylation of serine 1490 at the first PPPSP sequence (9). Cytosolic GSK3β has been proposed to be the kinase responsible for phosphorylating membrane-bound LRP6 receptor (10, 11), but it remains enigmatic how such phosphorylation is initiated on the plasma membrane.

G protein-coupled receptor kinases 5 and 6 (GRK5 and GRK6) are membrane-associated serine/threonine protein kinases, and they share sequence and functional similarities (12, 13). These two kinases are ubiquitously expressed and phosphorylate G protein-coupled receptors (GPCRs) upon agonist stimulation (12, 14). Such receptor phosphorylation initiates β-arrestin-mediated receptor desensitization, internalization, and signaling events (13). More and more data have been shown that β-arrestins are an important component in Wnt signaling (15–17). For example, β-arrestin2 can mediate Wnt5A-stimulated Frizzled 4 endocytosis via Dishevelled2 (17). However, whether GRKs can regulate Wnt signaling is unknown. Here, we report that GRK5 and GRK6 function as novel kinases responsible for LRP6 phosphorylation in Wnt signaling.

EXPERIMENTAL PROCEDURES

Plasmids, Antibodies, and Reagents—pcDNA3 LRP6 (human) was provided by Dr. J. Fred Hess (Merck, West Point, PA). Wnt luciferase reporter plasmid p8xTOPflash was obtained from Dr. Randall Moon (Washington University). LRP6 cyto-

[5] The abbreviations used are: LRP, low density lipoprotein receptor-related proteins; TM, transmembrane; GSK, glycogen synthase kinase; GPCR, G protein-coupled receptor; MOPS, 4-morpholinepropanesulfonic acid; shRNA, small hairpin RNA; RNAi, RNA interference; hpf, hour postfertilization; MO, morpholino; GRK, G protein-coupled receptor kinases; GAPDH, glyceraldehyde-3-phosphate dehydrogenase.

solic tail (LRP6-CT) and its M5 mutant genes from Dr. David Virshup (Duke-NUS Graduate Medical School) were cloned into pET30a (Stratagene) to express His$_6$-tagged LRP6-CT fusion protein in *Escherichia coli*. The following antibodies were used: anti-LRP6 phosphoserine 1490 antibody (Cell Signaling) with a 1:1000 dilution, anti-LRP6 antibody (clone C10, Santa Cruz Biotechnology) with a 1:1000 dilution, anti-β-catenin antibody (clone C2206, Sigma-Aldrich) with a 1:2000 dilution, anti-GAPDH antibody (clone 6C5, Abcam) with a 1:500 dilution, and anti-GRK5 or -GRK6 antibody (generated in our laboratories) with a 1:1000 dilution. Dickkopf-1 was purchased from R and D Systems. GRK5 was purified from Sf9 cells as described (18). Purified GRK6 and GSK3β were purchased from Upstate and Calbiochem, respectively. Both Wnt3A and control conditioned medium were produced from mouse L cells stably expressing mouse Wnt3A and wild type L cells (ATCC), respectively, according to the protocols described in ATCC.

Cell Culture, DNA Transfection, and Luciferase Reporter Assay—GRK6 knock-out MEFs were generated in our laboratory from GRK6 knock-out mice (19). HEK293 cells and MEF cells were maintained in MEM and Dulbecco's modified Eagle's medium, respectively, and both media were supplemented with 10% fetal bovine serum and 1% penicillin-streptomycin. DNA transfection was performed using Fugene 6 (Roche Applied Sciences) or Lipofectamine 2000 (Invitrogen) according to manufacturers' protocols. To conduct Wnt luciferase reporter assays, cells were transfected with plasmid DNAs expressing the genes of interest along with 0.25 μg of p8xTOPflash and 50 ng of an internal control *Renilla* luciferase plasmid (Promega) per well in a 12-well plate. The reporter assays were performed in triplicates, and the luciferase activity was measured using the Dual Luciferase kit from Promega.

Protein Purification—His$_6$-tagged LRP6 cytosolic tail and its M5 mutant protein were expressed in BL21DE3 pLysS (Stratagene), and purified using Invitrogen ProBond Resin nickel beads according to the manufacturer's procedure.

Kinase Phosphorylation Assay and Mass Spectrometry—Purified LRP6-CT protein was subjected to phosphorylation in the presence of [γ-^{32}P]ATP by purified GRK5, GRK6, and GSK3β in MOPS reaction buffer (20 mM MOPS pH 7.5, 10 mM MgCl$_2$, 2 mM EDTA, 1 mM dithiothreitol, and 60 μM non-radioactive ATP) at 30 °C for 1 h. The reactions were quenched by SDS loading buffer, resolved in 4–20% SDS-PAGE, and the phosphorylation signals were quantified by phosphorimager. For mass spectrometry to identify phosphorylation sites, nonradioactive (without addition of [γ-^{32}P]ATP) phosphorylation assays were performed under identical conditions as described above. A band corresponding to LRP6-CT protein was cut out from an SDS-PAGE gel, and mass spectrometry analysis was performed in the Taplin Biological Mass Spectrometry Facility (the laboratory of Dr. Steven Gygi) at Harvard University.

RNA Interference—Scramble lentiviral shRNA (Addgene plasmid 1864) and mouse GRK5 lentiviral shRNA (SHGLYC-TRCN0000022829) constructs were purchased from Addgene and Sigma, respectively. Lentivirus production and shRNA knock-down were performed according to protocols from Addgene. For GRK5 knock-down using siRNA, two mouse siRNAs
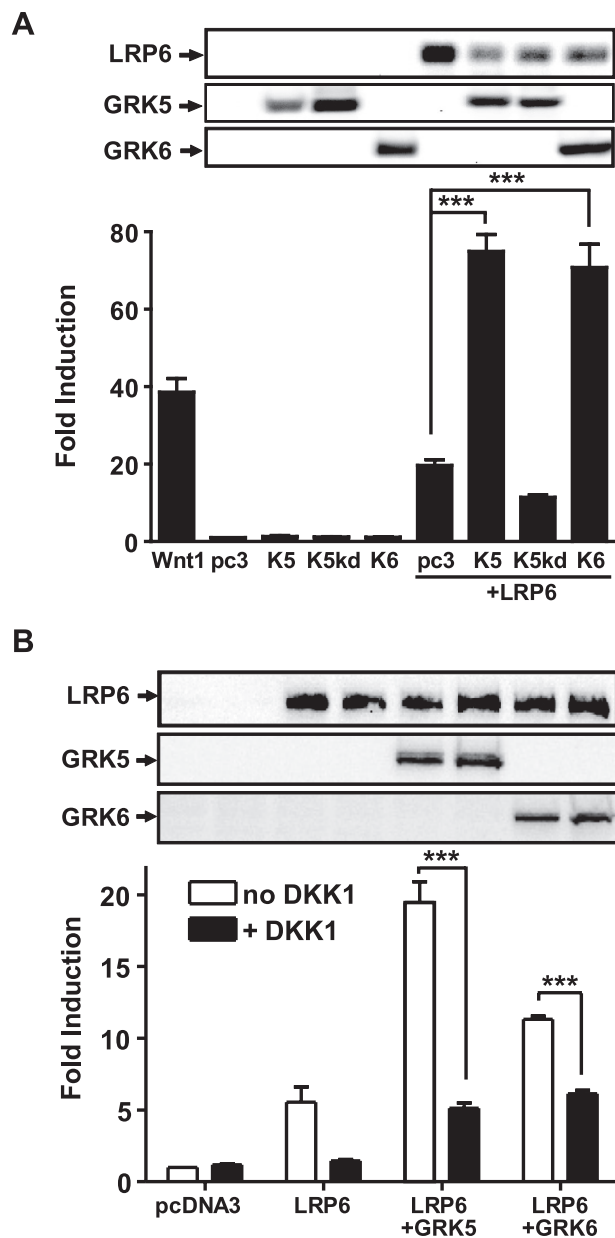
FIGURE 1. GRK5 and GRK6 enhance LRP6-mediated Wnt signaling. *A*, expression of GRK5 or GRK6 leads to increased Wnt signaling in the presence of LRP6 in HEK293 cells. In HEK293 cells expressing the TOPflash reporter, Wnt1 was expressed alone to serve as a positive control. Similarly, GRK5 (*K5*), GRK5 kinase-dead mutant (*K5kd*), or GRK6 (*K6*) was expressed alone or together with LRP6 for 48 h. TOPflash reporter luciferase activity was measured and normalized using a vector control (pc3, pcDNA3). Data are presented as fold induction relative to the empty vector. ***, $p < 0.0005$; Student's *t* test, $n = 3$. *B*, enhancement of Wnt signaling effect by GRK5 or GRK6 is inhibited by LRP6 antagonist DKK1. In HEK293 cells expressing the TOPflash reporter, cells were transfected with pcDNA3, LRP6 alone, LRP6 with GRK5 or GRK6 and then treated with 0.4 μg/ml of DKK1 for 30 h. TOPflash reporter activity is presented as fold induction relative to the empty vector. ***, $p < 0.0005$; Student's *t* test, $n = 3$.

(GRK5-1, 5′-AAGGACCATAGACAGAGATTA-3′; GRK5-2, 5′-AACCTGGCCTATGCCTATGAA-3′) were transfected into GRK6 knock-out MEFs using Lipofectamine 2000 according to the manufacturer's protocol. Human GRK5 siRNA, AAGGACCATAGACAGAGATTA; human GRK6 siRNA, AACAGTAGGTTTGTAGTGAGC, were used to deplete GRK5 or GRK6 levels in HEK293 cells, using Gene Silencer (Genlantis).
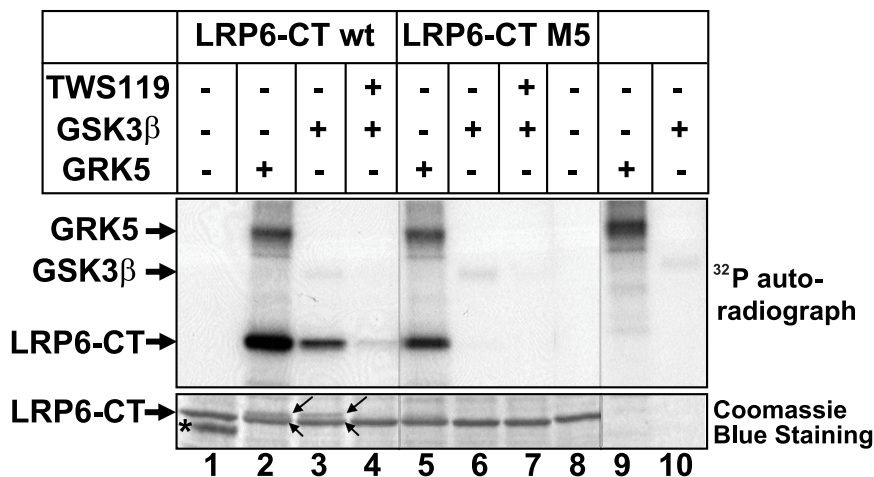
Cloning of Zebrafish LRP6 and GRK5—Zebrafish LRP6 (zLRP6) was amplified by PCR from cDNA of 12-somite stage (ss) embryos using the following primers: zLRP6-Forward 5′-CACCATGTATTGGACC-GACTGGG-3′ and zLRP6-Reverse 5′-TGAGGAGTCTGTGCAGGG-3′. Sequences upstream of the start codon were obtained from the current version of the zebrafish genome and verified by PCR using a high fidelity proofreading polymerase and sequencing. To obtain the complete coding sequence for zebrafish GRK5 (zGRK5), a sequence with significant homology to the mammalian GRK5 was identified by BLAST search of the Sanger zebrafish genome data base. A partial sequence was obtained by PCR from cDNA generated from 24 h postfertilization (hpf) embryos using the following primers: zGRK5-Forward 5′-AGCTCTCGAGATG-GCAGCGAACTGTGCA-3′ and zGRK5-Reverse 5′-AGCTCCGC-GGGGTTAAAATGTCTCCTT-ACGCGTCT-3′. 5′- and 3′-RACE PCRs were performed (First choice RLM RACE, Ambion) to obtain the full-length coding sequence and 5′-UTR. Full-length cDNA of zGRK5 was cloned into the pCS2+ vector, while zLRP6 was cloned into pcDNA3.1 using the TOPO directional cloning system (Invitrogen) to *in vitro*-transcribe capped mRNA for rescue experiments. Mutagenesis of full-length clones at the morpholino (MO) binding site was performed using the QuikChange Lightning Site-directed Mutagenesis kit (Stratagene). Sequences for zLRP6 (GQ903573) and zGRK5 (GQ903574) have been deposited in GenBank[TM].

Microinjection and Microscopy—All antisense morpholinos were designed and synthesized by Gene-Tools, LLC (Oregon) based upon submitted sequences. MOs were dissolved in double distilled water to final concentrations of 200–500 μM. Phenol Red was added to the solutions for better visualization during the injection. Approximately 3 nl of diluted MO were injected at the one-cell stage using
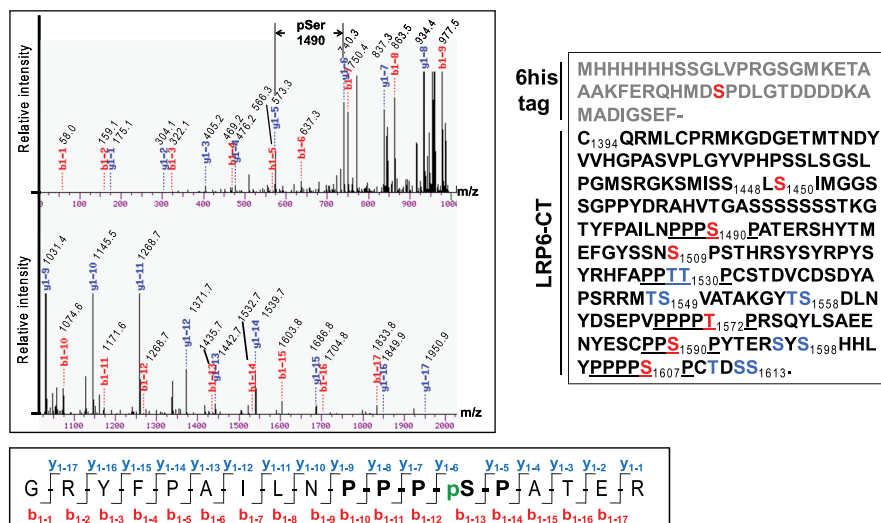
an Eppendorf Femtojet Microinjector. The sequences of the MOs are as follows: zLRP6 MO1: 5′-GATTGCTGCCATC-CATTCCGGCCCT-3′, zLRP6 MO2: 5′-TCTCTATTCTT-GGCTCCTCCCCCA-3′, zLRP6 5 nucleotide mismatch MO (zLRP6 CTRL MO): 5′-TTGAGATGTATAGACTCA-CTGTTGG-3′, zGRK5 MO1: 5′-TCGCTGCCATTGTTTC-GATCTCCAT-3′, zGRK5 MO2: 5′-GCTAAAAATCAGCC-AAGAAATGTGC-3′, zGRK5 5 nucleotide mismatch MO (zGRK5 CTRL MO): 5′-TCGGTGCGATTCTTTCCATCTG-CAT-3′. For rescue experiments, 10 pg (zLRP6) and 100 pg (zGRK5) of mRNA were injected per egg into the yolk. After microinjection, embryos were photographed using a Leica MZ16 dissection microscope equipped with a 4 megapixel monocamera and the OpenLab software. Measurements were carried out in OpenLab, and statistical analysis was performed in Prism (GraphPad Software).

Western Blots and in Situ Hybridization for Zebrafish Embryos—Lysates of 12 ss embryos were used for Western blots. For *in situ* hybridization, whole mount *in situ* hybridizations were performed according to standard techniques after PFA fixation at the indicated stages (20). For the detection of zGRK5 and zLRP6, two sets of non-overlapping DIG-labeled antisense RNA *in situ* probes were used. For analysis of wnt-responsive genes, *in situ* probes were generated from the following plasmids: An 811-bp fragment was amplified from 24 hpf cDNA using primers (Forward Axin2: 5′-GCCTAAAAGC-AAGGAGCAGAT, and Reverse Axin2: 5′-AAACTCATCAC-TGGCCCTTTT) based on *Danio rerio axin2* (NM_131561), and subcloned into pCRII using TOPO TA cloning (Invitrogen). The *in situ* probe for *cdx4* was prepared from a plasmid obtained from Zebrafish International Resource Center, clone cb546. To generate an *in situ* probe for *vent* a 407-bp fragment of accession number NM_131700 was amplified using a cDNA library of 6 hpf zebrafish embryo mRNA using the following primers: Forward vent 5′-TACCCAGCAAGTTCTCAGTGG, and Reverse vent 5′-AAAAACAGCGGGATAGAGGAA and cloned by TOPO TA cloning.

## RESULTS

GRK5 and GRK6 Enhance LRP6-mediated Wnt Signaling—We used the TOPflash (LEF/TCF) luciferase reporter to assess Wnt pathway activity regulated by GRK5 and GRK6. As a positive control, overexpression of either Wnt1 or LRP6 stimulated TOPflash reporter activity in HEK293 cells (Fig. 1*A*). Transfection of wild-type GRK5, a kinase-dead mutant of GRK5 (GRK5KD, GRK5 K215R mutant), or GRK6 had no effect on

enhancing TOPflash luciferase activity (Fig. 1*A*). However, co-expression of GRK5 or GRK6 with LRP6 greatly stimulated the TOPflash luciferase activity with an average 4-fold increase over that of LRP6 expressed alone, whereas GRK5KD did not enhance LRP6-mediated TOPflash luciferase activity (Fig. 1*A*). To confirm that LRP6 is specifically involved in GRK5 and GRK6-mediated Wnt signaling, we used Dickkopf-1 (DKK1), an LRP6 antagonist to inhibit LRP6 activity (21, 22). As shown in Fig. 1*B*, DKK1 inhibited the TOPflash luciferase activity stimulated by co-expression of GRK5 or GRK6 with LRP6, as well as the activity of LRP6 alone (Fig. 1*B*). These data suggest that GRK5 and GRK6 regulate canonical Wnt signaling in a kinase activity-dependent manner that also requires LRP6.

GRK5 and GRK6 Phosphorylate LRP6 at the PPPSP Motifs in Vitro—To demonstrate LRP6 phosphorylation by GRK5 and GRK6, we purified the His_6-tagged LRP6 cytoplasmic tail (LRP6-CT) from *E. coli*. The purified LRP6-CT was incubated with purified GRK5, GRK6, or GSK3β as control under phosphorylating conditions. As shown in Fig. 2*A*, GRK5 (*lane 2*) was a more effective kinase on LRP6-CT than GSK3β (*lane 3*), and the stoichiometry of LRP6-CT phosphorylation by GRK5 and GSK3β were ~1.2 and 0.3 phosphate/molecule under identical conditions (kinase/substrate molarity ratio is 1:5), respectively. Both GRK5 and GSK3β-mediated phosphorylation resulted in an additional slower mobility band of LRP6-CT (*lanes 2* and *3*, Coomassie Blue staining panel). In contrast, phosphorylation of a LRP6-CT mutant protein (LRP6-CT M5), in which all the serine and threonine residues within the five PPPSP motifs were mutated to alanine, was markedly impaired (about 50% decrease) in the presence of GRK5 (compare *lanes 2* and *5*) or eliminated in the presence of GSK3β (compare *lanes 3* and *6*). In addition, phosphorylation of LRP6-CT by GSK3β was inhibited by a GSK3β inhibitor TWS119 (23), which also partially inhibited GRK5 activity in our experiments (supplemental Fig. S1). Thus, GRK5 and GSK3β phosphorylate PPPSP motifs of soluble LRP6-CT in a similar manner, but GRK5 appears to be the more effective kinase. The novel observation that the GSK3β inhibitor TWS119 is also inhibitory to GRK5, coupled with our observation of functional similarity between GSK3β and GRK5 to phosphorylate the same PPPSP motifs on LRP6, further highlights the potential for close collaboration of these two kinases in the Wnt pathway. Similar to GRK5, GRK6 was also able to phosphorylate purified LRP6-CT *in vitro*, and this phosphory-

FIGURE 2. **GRK5 and GRK6 phosphorylate LRP6 at the PPPSP motifs *in vitro*.** *A*, *in vitro* phosphorylation of the LRP6 cytoplasmic tail by GRK5 and GSK3β. The *upper panel* shows partial amino acid sequences of the PPPSP motifs in the wild-type cytoplasmic tail of LRP6 (*LRP6-CT wt*) and the mutated PPPSP motifs (serine/threonine to alanine) in the LRP6-CT M5 mutant. PPPSP motifs are underlined and their serine/threonine or the corresponding mutations (alanines) are in *bold*. The *lower panels* show *in vitro* phosphorylation of wild-type LRP6-CT or LRP6-CT M5 mutant protein by GRK5 or GSK3β. Phosphorylated proteins were resolved by SDS-PAGE, subjected to γ-^{32}P autoradiography (*middle panel*) and colloidal Coomassie Blue staining (*bottom panel*). * symbol in *lane 1* indicates a prestained marker (29 kDa). *Arrowheads* in *lanes 2* and *3* indicate doublet bands of LRP6-CT in the SDS-PAGE gel. TWS119 is a GSK3β inhibitor, used at 20 μM. *B* and *C*, identification of phosphorylation sites on the cytoplasmic tail of LRP6 (*LRP6-CT*) phosphorylated by GRK5, GRK6, or GSK3β using mass spectrometry. The *left panels* in *B* show the mass spectrum, peak assignment, and amino acid sequence of the tryptic peptide containing serine 1490 (in the first PPPSP motif). The molecular weights of b-ion and y-ion are indicated. The *right panel* in *B* shows the entire amino acid sequence of His_6-tagged LRP6-CT, and the GRK5 phosphorylation sites identified by mass spectrometry. The amino acid sequence in *gray* is the His_6 tag sequence. The amino acid residues in *red* denote the phospho-serine/threonine residues that can be confidently identified, and the amino acid residues in *blue* indicates where phosphoserine/threonine has been identified within the tryptic peptide, but the precise position of phosphorylation cannot be assigned among multiple serine/threonine residues. PPPSP motifs are *underlined*. As summarized in *C*, the phosphorylation sites on LRP6-CT by GRK6 or GSK3β were also identified by mass spectrometry. "+" denotes phosphoserine/threonine; "−" denotes no phosphorylation. The experiments were independently repeated three times.
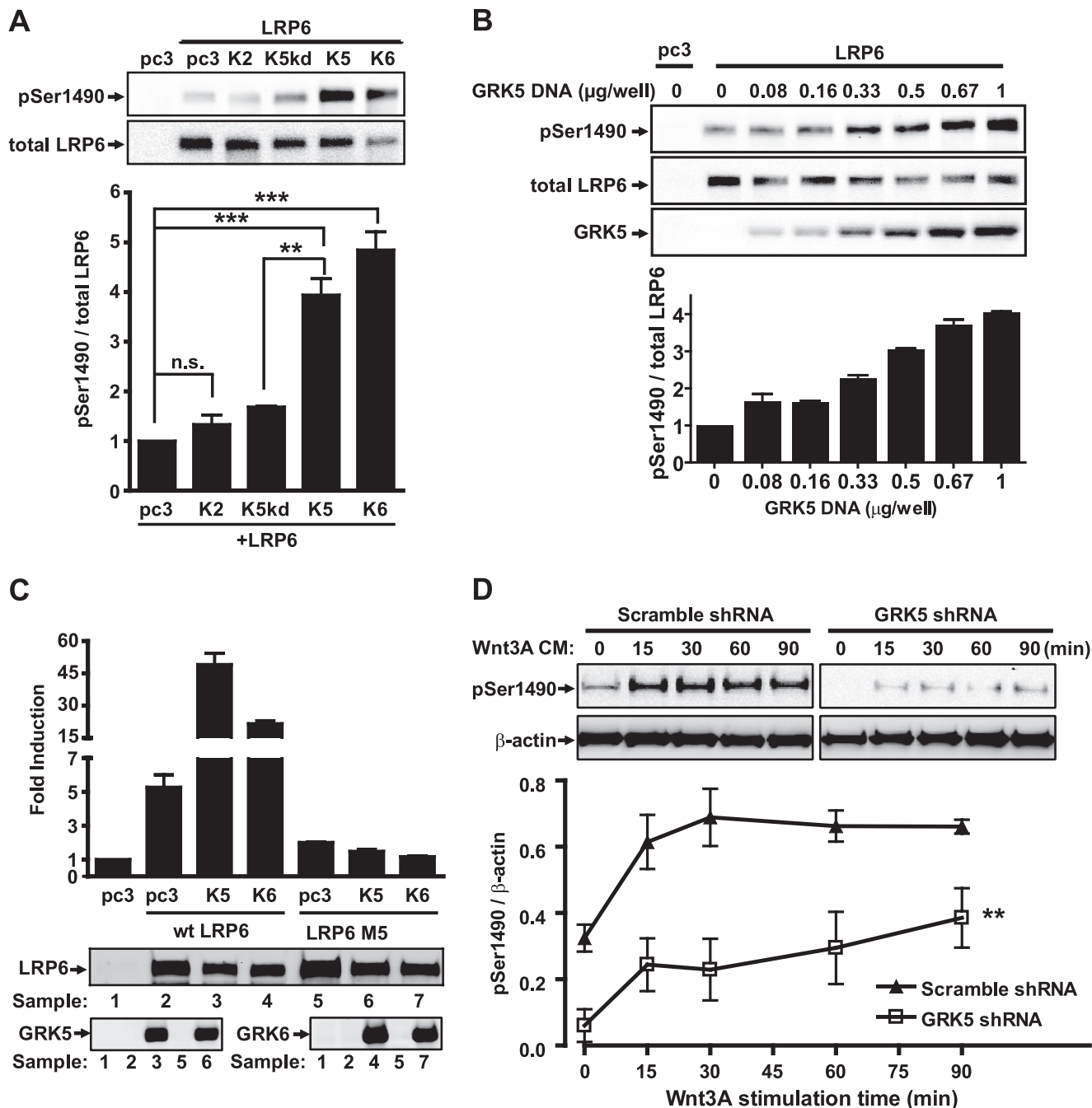
FIGURE 3. **GRK5 and GRK6 phosphorylate LRP6 and promote signaling in cellulo.** *A*, phosphorylation of LRP6 at serine 1490 by GRK5 or GRK6 in HEK293 cells. LRP6 was co-transfected with pcDNA3 (*pc3*) GRK2 (*K2*), GRK5 kinase-dead mutant (*K5kd*), GRK5 (*K5*), or GRK6 (*K6*) in HEK293 cells. 48 h post-transfection, LRP6 phosphorylation was detected by anti-pSer1490 immunoblots and normalized to total LRP6 expression. Representative blots are shown. The *bar graph* shows the quantitative summary of serine 1490 phosphorylation from three independent experiments. **, $p < 0.001$; and ***, $p < 0.0005$, Student's *t* test. *n.s.*, not significant. *B*, GRK5 phosphorylates LRP6 in a dose-dependent manner. Increasing amounts of GRK5 DNA as indicated were co-transfected with a fixed amount of LRP6 DNA into HEK293 cells. LRP6 phosphorylation was detected using an antibody against pSer-1490 of LRP6. Total LRP6 and GRK5 expression are shown below. The phosphorylation levels were normalized to total LRP6. *pc3* denotes pcDNA3. These data are representative of two independent experiments. *C*, PPPSP motifs are required for the enhancement of LRP6 signaling by GRK5/6. Full-length wild type (*wt*) LRP6 or LRP6 M5 mutant was expressed with pcDNA3 (*pc3*), GRK5, or GRK6 in HEK293 cells expressing TOPflash reporter. These data are representative of three separate experiments. *D*, knock-down of GRK5 level by GRK5 shRNA reduced Wnt3A-stimulated phosphorylation of endogenous LRP6. GRK6 knock-out MEF cells stably expressing scramble shRNA or GRK5 shRNA were stimulated with Wnt3A-conditioned medium (*Wnt3A CM*) for the time indicated. Endogenous LRP6 phosphorylation was detected by anti-pSer-1490 immunoblots and normalized to β-actin level as reported (24). Representative immunoblots are shown. Data from three independent LRP6 phosphorylation experiments are summarized in the bar graph. **, $p = 0.002$, *versus* scramble shRNA, Student's *t* test.

lation was reduced to about 50% when the LRP6-CT M5 mutant protein was used as a substrate (data not shown). We conclude that like GSK3β, both GRK5, and GRK6 can phosphorylate LRP6-CT within the PPPSP motifs, but also at other sites.

To determine the phosphorylation sites, we applied mass spectrometry to identify the phosphopeptides within the LRP6-CT phosphorylated by GRK5, GRK6, or GSK3β. In three independent mass spectrometry analyses, GRK5 phos-

phorylated all five PPPSP motifs in LRP6-CT, including the well-studied representative serine 1490 residue in the first PPPSP motif (Fig. 2, *B* and *C*). In addition to phosphorylation within the PPPSP motifs, serine 1450 and serine 1509 residues outside of PPPSP motifs were also phosphorylated by GRK5. These results agree with our observation that the LRP6-CT M5 mutant with unphosphorylable PPPSP motifs still can be phosphorylated by GRK5. Similarly, GRK6 phosphorylated three PPPSP motifs, including the first one containing serine 1490, as well as serine 1448 and serine 1509 outside these motifs (Fig. 2, *B* and *C*). GSK3β phosphorylated four PPPSP motifs, one of which contains serine 1490, as well as serine 1509 (Fig. 2, *B* and *C*). These data show that GRK5 and GRK6 are able to directly phosphorylate soluble LRP6-CT at the PPPSP motifs *in vitro*, just as GSK3β does. Besides the PPPSP motifs, these data also indicate that serine 1509 is a new common site that can be phosphorylated by these three kinases.

GRK5 and GRK6 Phosphorylate LRP6 in Cellulo—To study whether GRK5 and GRK6 phosphorylate LRP6 in cells, GRK5 or GRK6 was co-expressed with LRP6 in HEK293 cells. LRP6 phosphorylation was assessed using a phosphoserine 1490 (pSer-1490) antibody. Expression of GRK5 or GRK6 led to a 4–5-fold increase of serine 1490 phosphorylation (Fig. 3A), whereas expression of GRK5KD or GRK2, another member of the GRK family that is structurally and functionally distinct from GRK5 and GRK6 (12–14), had little or no effect (Fig. 3A). Increasing the amount of expressed GRK5 in cells led to proportional increases of LRP6 phosphorylation (Fig. 3B). These *in vitro* and *in cellulo* phosphorylation data identify GRK5 and GRK6 as membrane-associated kinases that can directly and specifically phosphorylate LRP6 at the PPPSP motifs.

Next we examined whether the PPPSP motifs are functionally important for GRK5- and GRK6-mediated LRP6 activation. We gener-

ated the full-length LRP6 M5 mutant, in which serine/threonine residues in all PPPSP motifs were mutated to alanine. In contrast to the GRK5 and GRK6-stimulated activity of wild-type LRP6, the LRP6 M5 mutant failed to respond to the expression of GRK5 or GRK6 (Fig. 3*C*) by increased TOPflash reporter activity, indicating that PPPSP motifs are indispensable for GRK5- and GRK6-mediated LRP6 activation.
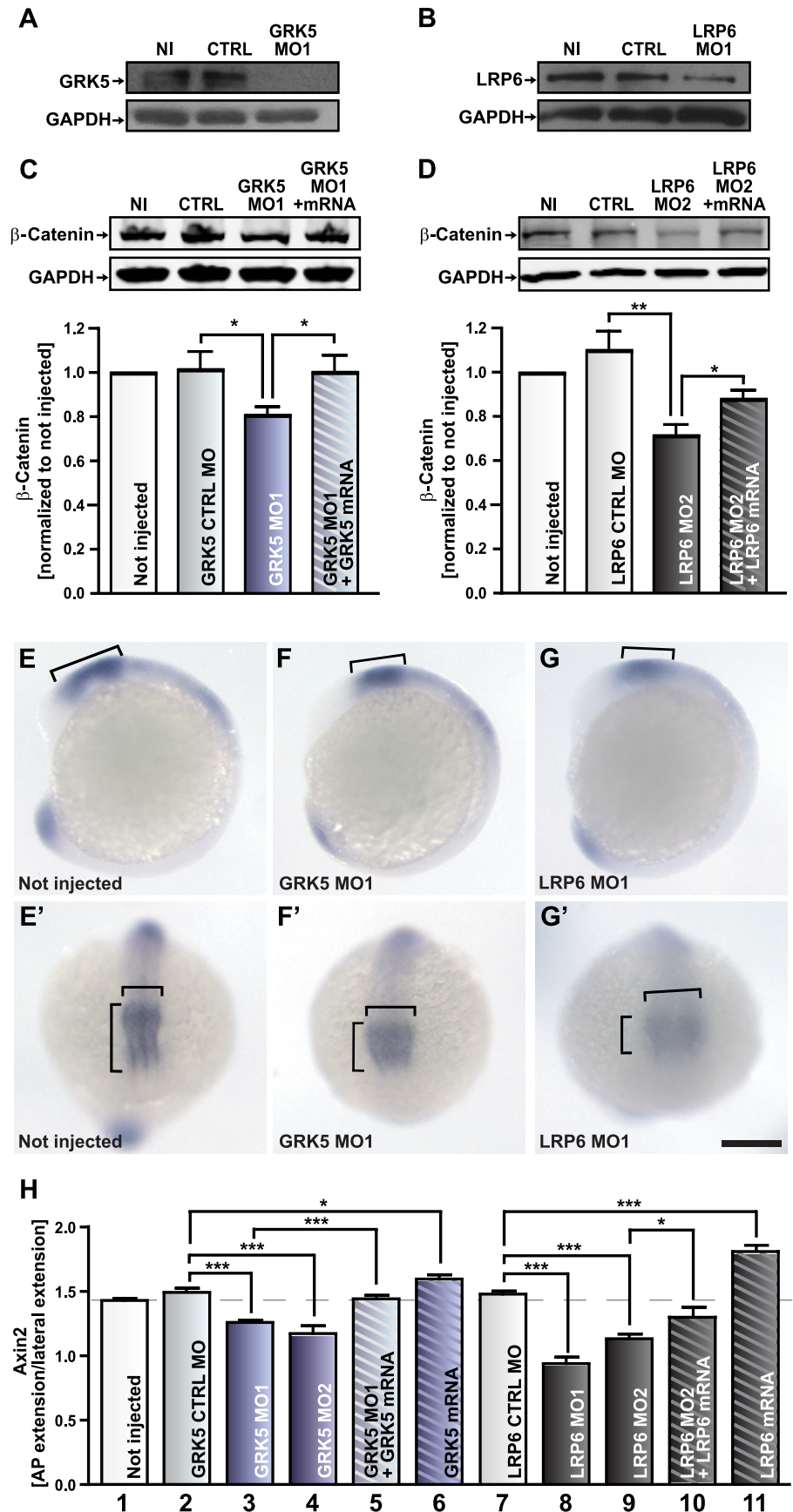
GRK5/6 Is Required for Wnt3A-stimulated Phosphorylation of Endogenous LRP6—Wnt3A stimulation can lead to LRP6 phosphorylation in the PPSP motifs (9). Next we investigated whether GRK5/6 was necessary for Wnt3A-stimulated LRP6 phosphorylation. To detect such phosphorylation of endogenous LRP6 (24), a GRK6 knock-out mouse embryonic fibroblast (MEF) cell line was generated (supplemental Fig. S2*A*) and used to study whether GRK5 was required for Wnt3A-stimulated endogenous LRP6 phosphorylation. In GRK6 knock-out MEFs, RNA interference (RNAi), including both GRK5 lentiviral shRNA (small hairpin RNA) (supplemental Fig. S2*B*) and GRK5 siRNA (small interfering RNA) (supplemental Fig. S3*A*), was employed to specifically knock-down endogenous GRK5 expression. The efficacy of RNAi knock-down was confirmed by Western blots using anti-GRK5 antibodies (supplemental Figs. S2*B* and S3*A*). In GRK6-knock-out MEFs infected with control/scramble lentiviral shRNA or transfected with control siRNA, Wnt3A treatment stimulated serine 1490 phosphorylation on endogenous LRP6 (Fig. 3*D* and supplemental Fig. S3, *B* and *C*). Knocking down GRK5 with either GRK5 lentiviral shRNA or GRK5 siRNA markedly reduced Wnt3A-stimulated serine 1490 phosphorylation (Fig. 3*D* and supplemental Fig. S3, *B* and *C*), indicating that GRK5 plays an important role in regulating Wnt3A-stimulated LRP6 phosphorylation.

GRK5 Modulates Wnt Signaling in Zebrafish, Analogous to LRP6—We turned to a whole animal model, the zebrafish, to assess the physiological relevance of LRP6 phosphorylation by GRK5/6. We cloned the zebrafish homologs of mammalian GRK5 and LRP6 (zGRK5 and zLRP6) and performed *in situ* hybridization at several developmental stages, finding an overlapping expression pattern of zGRK5 and zLRP6 (supplemental Fig. S4, *A–F*). During somitogenesis, zGRK5 and zLRP6 are ubiquitously expressed (supplemental Fig. S4, *A* and *D*). At later stages, zLRP6 expression is restricted to the diencephalon, the tegmentum and the hindbrain (supplemental Fig. S4, *E* and *F*). Although zGRK5 appears to be ubiquitously expressed in the brain at 24 hpf (supplemental Fig. S4*B*), it could be detected in a more discrete pattern at 48 hpf, partially overlapping the expression of zLRP6 (supplemental Fig. S4*C*).

To test for an involvement of zGRK5 in canonical Wnt signaling, we designed two different translation blocking antisense morpholinos (MO) for zGRK5 and for zLRP6. Injection of either zGRK5 MO into the yolk of one-cell stage embryos specifically down-regulated zGRK5 protein expression, as assessed in Western blots, whereas a 5-nucleotide mismatch MO (zGRK5 CTRL) did not (Fig. 4*A*). Similarly, injection of either zLRP6 MO diminished protein levels of zLRP6 in 12 ss embryos (Fig. 4*B*).

To assess the effect of zGRK5 on canonical Wnt signaling, we analyzed β-catenin levels in whole embryo lysates at the 12 ss. We detected lowered levels of β-catenin in zGRK5 morphants, whereas in CTRL morphants β-catenin levels were not altered (Fig. 4*C*). In Fig. 4*D*, we repeated the same experiment using zebrafish injected with zLRP6 MO as a control and as a model for diminished Wnt signaling. As expected, β-catenin levels were reduced in lysates of embryos injected with the translation blocking zLRP6 MO, but not when injected with a 5-nucleotide mismatch MO (zLRP6 CTRL) (Fig. 4*D*). In both zGRK5 or zLRP6 MO-injected embryos, the reduction of β-catenin accumulation could be partially reversed by co-injection of capped mRNA bearing silent mutations in the MO binding site (Fig. 4, *C* and *D*).

In zebrafish, *axin2* transcription has been used as readout for Wnt signaling (25, 26). When we analyzed zebrafish injected with either zGRK5 or zLRP6 MOs, the *axin2*-positive area in the brain extended significantly less anteriorly in GRK5 MO-injected fish (Fig. 4, *F* and *F′* and supplemental Fig. S4, *H* and *H′*) or LRP6 MO-injected fish (Fig. 4, *G* and *G′* and supplemental Fig. S4, *L* and *L′*), when compared with uninjected or CTRL MO-injected fish (Fig. 4, *E* and *E′*, and supplemental Fig. S4, *G*, *G′*, *K*, and *K′*). As summarized in Fig. 4*H*, zGRK5 knock-down (Fig. 4*H*, bars 3 and 4, compared with bar 2) mimics the phenotype of zLRP6 knock-down (Fig. 4*H*, bars 8 and 9, compared with bar 7), which translates to a significant reduction in the anterior extension of *axin2* expression in the developing brain. Co-injection of low doses of capped mRNA bearing silent mutations for the respective MO binding sites rescued the antisense MO phenotype (Fig. 4*H*, bars 5 and 10). In accordance with the results obtained in cells, overexpression of zGRK5 by injection of mRNA enhanced Wnt signaling (Fig. 4*H*, bar 6), although to a lesser extent than zLRP6 mRNA did (Fig. 4*H*, bar 11) (see also supplemental Fig. S4, *G–N′*).

We also examined the transcription of *cdx4* (27, 28) and *vent* (29, 30) genes, which have also been used as readouts for Wnt signaling in zebrafish embryos. Similar to the zebrafish em-

FIGURE 4. **GRK5 modulates the expression of β-catenin and axin2 in Wnt signaling in zebrafish, analogous to LRP6.** *A* and *B*, representative Western blots to show knock-down of GRK5 (*A*) and LRP6 (*B*) levels in zebrafish. *NI*, not injected wild-type zebrafish; *CTRL*, zebrafish injected with control morpholino; *GRK5 MO1*, zebrafish injected with zGRK5 morpholino 1; *LRP6 MO1*, zebrafish injected with translation blocking MO1 for zLRP6. GAPDH is used as loading control. *C*, representative Western blots and for β-catenin and GAPDH using embryos, which were either uninjected (*NI*) or injected with CTRL MO (*CTRL*), translation-blocking zGRK5 MO1 (*GRK5 MO1*), or co-injected with zGRK5 MO1 and zGRK5 mRNA (*GRK5 MO1+mRNA*). The graph shows the average of densitometric quantitation of six independent experiments. *Bars* represent mean ± S.E. *, $p < 0.05$; Student's *t* test. *D*, Western blots of wild-type zebrafish (*NI*) and zebrafish injected with control morpholino (*CTRL*), zLRP6 morpholino (*LRP6 MO2*), or co-injected with zLRP6 MO2 and mRNA (*LRP6 MO2+mRNA*) to assess accumulation of β-catenin as controlled to GAPDH. Bar graph summarizes four independent experiments as mean ± S.E.; *, $p < 0.04$ (zLRP6 MO2 *versus* zLRP6 MO2 + zLRP6 mRNA); **, $p < 0.001$ (zLRP6 CTRL MO *versus* zLRP6 MO2), Student's *t* test. *E–G′*, *in situ* hybridizations for *axin2* shown for zebrafish embryos either not injected (*E* and *E′*) or injected with either zGRK5 MO1 (*F* and *F′*) or zLRP6 MO1 (*G* and *G′*). The same embryos are depicted in both lateral view (*E*, *F*, and *G*) and from the top (*E′*, *F′*, and *G′*). *Brackets* indicate the limits for measurements of anterior-posterior extensions of the *axin2*-positive area in the brain and of lateral extensions, respectively. *H*, graphical representation of *axin2* expression upon knock-down of zGRK5 or zLRP6 as ratios of anterior-posterior extension over lateral extension ($n = 17–122$ fish per condition). All *axin2* experiments were carried out at the 12 somite stage. *, $p < 0.05$; ***, $p < 0.0001$, Student's *t* test. *Scale bar*, 200 μm.
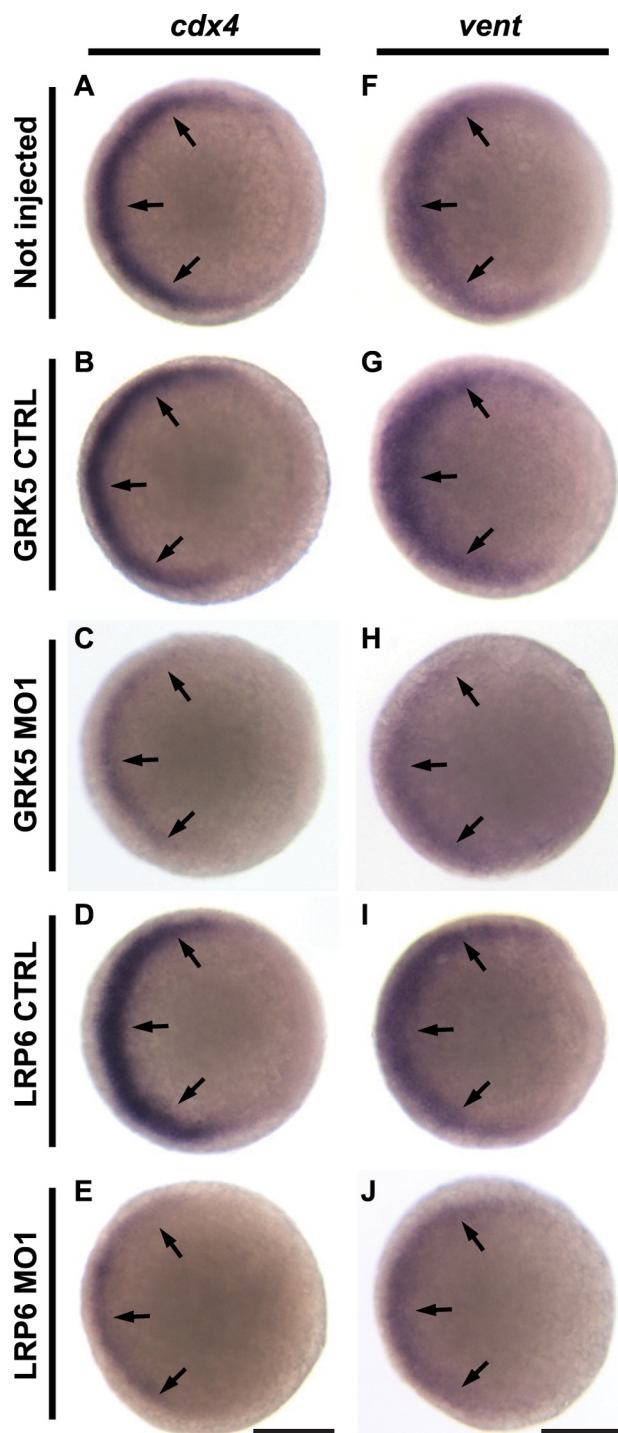
FIGURE 5. **GRK5 modulates the expression of *cdx4* and *vent* in Wnt signaling in zebrafish, analogous to LRP6.** *A–J, in situ* hybridizations for *cdx4* (*A–E*) and *vent* (*F–J*) shown for zebrafish embryos either not injected (*A* and *F*) or injected with zGRK5 CTRL MO (*B* and *G*), zGRK5 MO1 (*C* and *H*), zLRP6 CTRL MO (*D* and *I*), or zLRP6 MO1 (*E* and *J*) at 30–50% epiboly. The embryos are depicted in the animal view with dorsal to the *right*. *Arrowheads* point to the expression domains of *cdx4* or *vent*. *Scale bar*, 200 μm.

bryos injected with LRP6 MO (Fig. 5, *E* and *J*), the zebrafish embryos injected with zGRK5 MO show significantly reduced *cdx4* (Fig. 5*C*) and *vent* (Fig. 5*H*) transcription as compared to zebrafish embryos not injected (Fig. 5, *A* and *F*) or injected with control MOs (Fig. 5, *B*, *G*, *D*, and *I*). Taken together, these results demonstrate that GRK5 positively regulates LRP6-de-

pendent Wnt signal transduction in zebrafish, assessed both at the post-translational level (measuring β-catenin accumulation) and at the transcriptional level (assessing *axin2, cdx4*, and *vent* as Wnt-responsive genes).

DISCUSSION

In this study, we have provided biochemical and physiological evidence to demonstrate that widely expressed GRK5 and GRK6 have an unexpected and important function during Wnt signaling as membrane-bound kinases phosphorylating LRP6. The classical role of GRK5 and GRK6 is to phosphorylate activated GPCRs, initiating β-arrestin binding for receptor desensitization, internalization, and signaling (12–14). Our findings that GRK5 and GRK6 phosphorylate the single membrane-spanning receptor LRP6 on defined serine/threonine sites (*i.e.* serine 1490) within proline-rich PPPSP motifs and thereby activate LRP6 are important and interesting in two respects. First, this result extends the range of receptor families, in addition to GPCRs, that can be phosphorylated and regulated by GRK5 and GRK6. Furthermore, instead of having an inhibitory role as in classical G-protein mediated signaling, GRK5 and GRK6 might have a stimulatory role in Wnt/LRP6 signaling. This suggests that GRK5 and GRK6 may have much broader roles than are currently appreciated. Second, our data provide a novel mechanism for LRP6 phosphorylation and regulation at the plasma membrane. Previously, we have shown that β-arrestin2 is recruited to the plasma membrane to bind to Frizzled through Dishevelled and thereby regulates Frizzled function (17). Because GRKs and β-arrestins function in concert in regulating GPCRs, it is quite surprising that GRK5/6 and β-arrestin2 participate in regulating Wnt signaling by separate means, delineating their distinct and independent functions. Additional studies will be needed to clarify how Wnt-induced activation of LRP6 leads to GRK5/6 recognition of the receptor as substrate.

In addition, the data presented here also solve a paradox within the current model of LRP6 phosphorylation by GSK3β in the cytoplasm. In a cellular system that included an artificially membrane-associated GSK3β mutant, cytosolic GSK3β was proposed to be recruited to the plasma membrane through the adaptor protein axin to phosphorylate LRP6 at the PPPSP motifs (11). However, for axin to bind LRP6, the PPPSP motifs must first be phosphorylated, at a time when GSK3β is still in the cytoplasm (10, 11). Therefore, at least the initiation of both PPPSP phosphorylation and axin translocation to membrane LRP6 would be expected to be GSK3β independent. Our finding that GRK5 and GRK6 function as LRP6 kinases presents a straightforward mechanism for understanding LRP6 phosphorylation and activation, as these kinases are membrane bound already and are therefore available to initiate LRP6 by phosphorylation to promote subsequent axin/GSK3β binding. In addition, it has been recently shown that parathyroid hormone (PTH) and its receptor (PTHR), a GPCR that can be phosphorylated by GRK5 (31), regulates phosphorylation of LRP6 serine 1490 to activate LRP6 in a Wnt-independent fashion (32). However, the kinase responsible for PTH/PTHR-mediated LRP6 phosphorylation is unknown. Our studies might also suggest a role for GRK5 and GRK6 in PTH/PTHR-mediated LRP6 phosphorylation.

Taken together, our results provide new insight into the actions of GRK5 and GRK6. By phosphorylating LRP6 on PPPSP motifs they contribute to Wnt signaling, a pathway critical for basic biological processes in cells and during embryonic development.

REFERENCES

1. Pinson, K. I., Brennan, J., Monkley, S., Avery, B. J., and Skarnes, W. C. (2000) *Nature* **407,** 535–538
2. Tamai, K., Semenov, M., Kato, Y., Spokony, R., Liu, C., Katsuyama, Y., Hess, F., Saint-Jeannet, J. P., and He, X. (2000) *Nature* **407,** 530–535
3. van Amerongen, R., Mikels, A., and Nusse, R. (2008) *Sci. Signal* **1,** re9
4. Wehrli, M., Dougan, S. T., Caldwell, K., O'Keefe, L., Schwartz, S., Vaizel-Ohayon, D., Schejter, E., Tomlinson, A., and DiNardo, S. (2000) *Nature* **407,** 527–530
5. He, X., Semenov, M., Tamai, K., and Zeng, X. (2004) *Development* **131,** 1663–1677
6. Moon, R. T., Kohn, A. D., De Ferrari, G. V., and Kaykas, A. (2004) *Nat. Rev. Genet* **5,** 691–701
7. Fuerer, C., Nusse, R., and Ten Berge, D. (2008) *EMBO Rep.* **9,** 134–138
8. Davidson, G., Wu, W., Shen, J., Bilic, J., Fenger, U., Stannek, P., Glinka, A., and Niehrs, C. (2005) *Nature* **438,** 867–872
9. Tamai, K., Zeng, X., Liu, C., Zhang, X., Harada, Y., Chang, Z., and He, X. (2004) *Mol. Cell* **13,** 149–156
10. Zeng, X., Huang, H., Tamai, K., Zhang, X., Harada, Y., Yokota, C., Almeida, K., Wang, J., Doble, B., Woodgett, J., Wynshaw-Boris, A., Hsieh, J. C., and He, X. (2008) *Development* **135,** 367–375
11. Zeng, X., Tamai, K., Doble, B., Li, S., Huang, H., Habas, R., Okamura, H., Woodgett, J., and He, X. (2005) *Nature* **438,** 873–877
12. Pitcher, J. A., Freedman, N. J., and Lefkowitz, R. J. (1998) *Annu. Rev. Biochem.* **67,** 653–692
13. Premont, R. T., and Gainetdinov, R. R. (2007) *Annu. Rev. Physiol.* **69,** 511–534
14. Premont, R. T., Inglese, J., and Lefkowitz, R. J. (1995) *Faseb. J.* **9,** 175–182
15. Bryja, V., Gradl, D., Schambony, A., Arenas, E., and Schulte, G. (2007) *Proc. Natl. Acad. Sci. U.S.A.* **104,** 6690–6695
16. Chen, W., Hu, L. A., Semenov, M. V., Yanagawa, S., Kikuchi, A., Lefkowitz, R. J., and Miller, W. E. (2001) *Proc. Natl. Acad. Sci. U.S.A.* **98,** 14889–14894
17. Chen, W., ten Berge, D., Brown, J., Ahn, S., Hu, L. A., Miller, W. E., Caron, M. G., Barak, L. S., Nusse, R., and Lefkowitz, R. J. (2003) *Science* **301,** 1391–1394
18. Premont, R. T., Koch, W. J., Inglese, J., and Lefkowitz, R. J. (1994) *J. Biol. Chem.* **269,** 6832–6841
19. Gainetdinov, R. R., Bohn, L. M., Sotnikova, T. D., Cyr, M., Laakso, A., Macrae, A. D., Torres, G. E., Kim, K. M., Lefkowitz, R. J., Caron, M. G., and Premont, R. T. (2003) *Neuron* **38,** 291–303
20. Thisse, C., and Thisse, B. (2008) *Nat. Protoc.* **3,** 59–69
21. Bafico, A., Liu, G., Yaniv, A., Gazit, A., and Aaronson, S. A. (2001) *Nat. Cell Biol.* **3,** 683–686
22. Mao, B., Wu, W., Li, Y., Hoppe, D., Stannek, P., Glinka, A., and Niehrs, C. (2001) *Nature* **411,** 321–325
23. Ding, S., Wu, T. Y., Brinker, A., Peters, E. C., Hur, W., Gray, N. S., and Schultz, P. G. (2003) *Proc. Natl. Acad. Sci. U.S.A.* **100,** 7632–7637
24. Wei, Q., Yokota, C., Semenov, M. V., Doble, B., Woodgett, J., and He, X. (2007) *J. Biol. Chem.* **282,** 15903–15911
25. Gerdes, J. M., Liu, Y., Zaghloul, N. A., Leitch, C. C., Lawson, S. S., Kato, M., Beachy, P. A., Beales, P. L., DeMartino, G. N., Fisher, S., Badano, J. L., and Katsanis, N. (2007) *Nat. Genet.* **39,** 1350–1360
26. Weidinger, G., Thorpe, C. J., Wuennenberg-Stapleton, K., Ngai, J., and Moon, R. T. (2005) *Curr. Biol.* **15,** 489–500
27. Shimizu, T., Bae, Y. K., Muraoka, O., and Hibi, M. (2005) *Dev. Biol.* **279,** 125–141
28. Davidson, A. J., Ernst, P., Wang, Y., Dekens, M. P., Kingsley, P. D., Palis, J., Korsmeyer, S. J., Daley, G. Q., and Zon, L. I. (2003) *Nature* **425,** 300–306
29. Ramel, M. C., and Lekven, A. C. (2004) *Development* **131,** 3991–4000
30. Ramel, M. C., Buckles, G. R., Baker, K. D., and Lekven, A. C. (2005) *Dev. Biol.* **287,** 237–248
31. Dicker, F., Quitterer, U., Winstel, R., Honold, K., and Lohse, M. J. (1999) *Proc. Natl. Acad. Sci. U.S.A.* **96,** 5476–5481
32. Wan, M., Yang, C., Li, J., Wu, X., Yuan, H., Ma, H., He, X., Nie, S., Chang, C., and Cao, X. (2008) *Genes Dev.* **22,** 2968–2979